Hindawi
International Journal of Antennas and Propagation
Volume 2019, Article ID 6343641, 6 pages
https://doi.org/10.1155/2019/6343641

Research Article

Well-Designed Termination Wall of Perfectly Matched Layers for ATS-FDTD Method

Ju Ge, Liping Gao, and Rengang Shi

College Of Science, China University of Petroleum (Huadong), QingDao, 266580, China

Correspondence should be addressed to Rengang Shi; shirg@upc.edu.cn

Received 8 February 2019; Accepted 24 April 2019; Published 2 June 2019

Academic Editor: Luciano Tarricone

This paper presents a well-designed termination wall for the perfectly matched layers (PML). This termination wall is derived from Mur's absorbing boundary condition (ABC) with special difference schemes. Numerical experiments illustrate that PML and the termination wall works well with ATS-FDTD(Shi et al. 2015). With the help of termination wall, perfectly matched layers can be decreased to two layers only; meanwhile, the reflection error still reaches -60[dB] when complex waveguide is simulated by ATS-FDTD.

1. Introduction

It is well known that the perfectly matched layers (PML) [1–4] are wildly used for simulating Maxwell's equations in unbounded domain. The overall performance of PML depends on its all parameters, and the optimal parameters have been studied by many scientists [5–9].

To avoid causing much rebound at PEC, the traditional termination wall of PML, the PML are improved by some termination walls [8–11]. In [8], a lossy version of the one-way Engquist Majda ABC was used for the termination of magnetic-field component of PML and the electric-field component of PML was terminated by an according transverse impedance with specific direction θ_m, which lead to the inconvenience of this method. In [9–11], unified lossy version of Mur's second-order ABC and dispersive boundary condition were developed to be the PML termination for wave equation which could be derive from Maxwell equations. The thickness of PML is still a restriction; none of the above improved PML can reach optimal thickness, two layers, with good performance.

In this paper, a special single-layer Mur's ABC is designed as the PML termination for solving 2D Maxwell equations by ATS-FDTD [12] method. The staggered grids are used in this paper and the electromagnetic field components are placed on the boundary of each cell, $E^n_{x_{i,j+1/2}}, E^n_{y_{i+1/2,j}}$ and $H^n_{z_{i,j}}$, which is different from the traditional Yee's grid [13]. The magnetic-field component of PML is terminated by first-order Mur's ABC where the difference schemes will be designed very differently. This termination wall, PML-ABC, is very convenient and effective to be implemented with the ATS-FDTD method to solve Maxwell equation.

2. The PML-ABC and ATS-FDTD

The equations of PML [8] are given by

$$\begin{aligned}
\varepsilon\frac{\partial E_x}{\partial t} + \sigma_y E_x &= \frac{\partial\left(H_{zx}+H_{zy}\right)}{\partial y}\\
\varepsilon\frac{\partial E_y}{\partial t} + \sigma_x E_y &= -\frac{\partial\left(H_{zx}+H_{zy}\right)}{\partial x}\\
\mu\frac{\partial H_{zx}}{\partial t} + \sigma_{mx} H_{zx} &= -\frac{\partial E_y}{\partial x}\\
\mu\frac{\partial H_{zy}}{\partial t} + \sigma_{my} H_{zy} &= \frac{\partial E_x}{\partial y}
\end{aligned} \tag{1}$$

where (and in what follows) $H_z = H_{zx} + H_{zy}$ in the PML. σ_x, σ_y and σ_{mx}, σ_{my} are the electric and magnetic

conductivities of the PML, which satisfy the impedance matching condition

$$\frac{\sigma_x}{\varepsilon} = \frac{\sigma_{mx}}{\mu}, \qquad \frac{\sigma_y}{\varepsilon} = \frac{\sigma_{my}}{\mu}. \tag{2}$$

The boundaries of PML are given by Mur's ABC:

$$\begin{aligned} &\frac{\partial H_{zx}}{\partial x} - \frac{1}{c}\frac{\partial H_{zx}}{\partial t} = 0, \quad \text{on left boundary} \\ &\frac{\partial H_{zx}}{\partial x} + \frac{1}{c}\frac{\partial H_{zx}}{\partial t} = 0, \quad \text{on right boundary} \\ &\frac{\partial H_{zy}}{\partial y} - \frac{1}{c}\frac{\partial H_{zy}}{\partial t} = 0, \quad \text{on below boundary} \\ &\frac{\partial H_{zy}}{\partial y} + \frac{1}{c}\frac{\partial H_{zy}}{\partial t} = 0, \quad \text{on upper boundary} \end{aligned} \tag{3}$$

which $c = 1/\sqrt{\varepsilon\mu}$ is the speed of light in vacuum.

This paper uses the staggered grid technique:

$$\begin{aligned} x_i &= ih, \\ x_{i+1/2} &= x_i + \frac{h}{2}, \\ y_{j+1/2} &= y_j + \frac{h}{2}, \\ y_j &= jh, \\ t^n &= n\Delta t, \\ t^{n+1/2} &= t^n + \frac{\Delta t}{2}, \end{aligned} \tag{4}$$

where h and Δt are the size of grid. By ATS-FDTD method, the approximations can be expressed as

$$E^n_{x_{i,j+1/2}} = \sum_{k=0}^{K} C^k_{x_{i,j+1/2}} \Delta t^k \tag{5}$$

$$E^n_{y_{i+1/2,j}} = \sum_{k=0}^{K} C^k_{y_{i+1/2,j}} \Delta t^k \tag{6}$$

$$H^n_{z_{i,j}} = \sum_{k=0}^{K} C^k_{z_{i,j}} \Delta t^k \tag{7}$$

$$H^n_{zx_{i,j}} = \sum_{k=0}^{K} C^k_{zx_{i,j}} \Delta t^k \tag{8}$$

$$H^n_{zy_{i,j}} = \sum_{k=0}^{K} C^k_{zy_{i,j}} \Delta t^k \tag{9}$$

where $C^0_{x_{i,j+1/2}} = E^{n-1}_{x_{i,j+1/2}}$, $C^0_{y_{i+1/2,j}} = E^{n-1}_{y_{i+1/2,j}}$, $C^0_{z_{i,j}} = H^{n-1}_{z_{i,j+1/2}}$ are the value at the former time level and K is positive integer and should be determined by

$$\left| \sum_{k=0}^{K} \frac{(-4\Delta t/h)^k}{k!} \right| < 1. \tag{10}$$

The unknown coefficients $C^k_{x_{i,j+1/2}}$, $C^k_{y_{i+1/2,j}}$, $C^k_{z_{i,j}}$, $C^k_{zx_{i,j}}$, and $C^k_{zy_{i,j}}$ are determined by recursion formulas (11)-(21).

In vacuum, the unknown coefficients are obtained by

$$\varepsilon C^{k+1}_{x_{i,j+1/2}} = \frac{\delta_y C^k_{z_{i,j+1/2}}}{k+1} \qquad \begin{matrix} i = d+1, \cdots, I-1-d \\ j = d, \cdots, J-1-d \end{matrix} \tag{11}$$

$$\varepsilon C^{k+1}_{y_{i+1/2,j}} = -\frac{\delta_x C^k_{z_{i+1/2,j}}}{k+1} \qquad \begin{matrix} i = d, \cdots, I-1-d \\ j = d+1, \cdots, J-1-d \end{matrix} \tag{12}$$

$$\mu C^{k+1}_{z_{i,j}} = \frac{\delta_y C^k_{x_{i,j}} - \delta_x C^k_{y_{i,j}}}{k+1} \qquad \begin{matrix} i = d+1, \cdots, I-1-d \\ j = d+1, \cdots, J-1-d \end{matrix} \tag{13}$$

where I, J, and d are positive integer, I and J are the grid number in x and y direction, separately, d is the thickness of PML, and δ_x and δ_y are differential operator, such as $\delta_x C^k_{y_{i,j}} = (C^k_{y_{i+1/2,j}} - C^k_{y_{i-1/2,j}})/h$; the other can be similarly defined.

The coefficients $C^k_{x_{i,j+1/2}}$ in PML are given by

$$\varepsilon C^{k+1}_{x_{i,j+1/2}} = \frac{\left(-\sigma_y C^k_{x_{i,j+1/2}} + \delta_y \left(C^k_{zx_{i,j}} + C^k_{zy_{i,j}}\right)\right)}{(k+1)} \qquad \begin{matrix} i = 0, \cdots, I, \ \ j = 0, \cdots, d-1; J-d, \cdots, J-1 \\ i = 0, \cdots, d; I-d, \cdots, I, \ \ j = d, \cdots, J-d-1 \end{matrix} \tag{14}$$

The coefficients of $E^n_{y_{i+1/2,j}}$ in PML are given by

$$C^{k+1}_{y_{i+1/2,j}} = \frac{\left(-\sigma_x C^k_{y_{i+1/2,j}} - \delta_x \left(C^k_{zx_{i,j}} + C^k_{zy_{i,j}}\right)\right)}{(k+1)} \qquad \begin{matrix} i = 0, \cdots, d-1; I-d, \cdots, I-1, \ \ j = 0, \cdots, J \\ i = d, \cdots, I-d-1, \ \ j = 0, \cdots, d; J-d, \cdots, J \end{matrix} \tag{15}$$

From the equation in (1), the schemes for coefficients of $H^n_{zx_{i,j}}$ and $H^n_{zy_{i,j}}$ in PML are written as

$$\mu C^{k+1}_{zx_{i,j}} = \frac{\left(-\sigma_{mx} C^k_{zx_{i,j}} - \delta_x C^k_{y_{i+1/2,j}}\right)}{(k+1)} \quad \begin{matrix} i = 1, \cdots, d; I-d, \cdots, I-1, \ j = 0, \cdots, J \\ i = d+1, \cdots, I-1-d, \ j = 0, \cdots, d; J-d, \cdots, J \end{matrix} \tag{16}$$

$$\mu C^{k+1}_{zy_{i,j}} = \frac{\left(-\sigma_{my} C^k_{zy_{i,j}} + \delta_y C^k_{x_{i,j+1/2}}\right)}{(k+1)} \quad \begin{matrix} j = 1, \cdots, d; J-d, \cdots, J-1, \ i = 0, \cdots, I \\ j = d+1, \cdots, J-1-d, \ i = 0, \cdots, d; I-d, \cdots, I \end{matrix} \tag{17}$$

The schemes for coefficients of H_{zx} and H_{zy} at the Mur's ABC are given by

$$\mu C^{k+1}_{zx_{0,j}} = \frac{-3C^k_{zx_{0,j}} + 4C^k_{zx_{1,j}} - C^k_{zx_{2,j}}}{2h\,(k+1)} \quad j = 0, \cdots, J \tag{18}$$

$$\mu C^{k+1}_{zx_{I,j}} = \frac{-3C^k_{zx_{I,j}} + 4C^k_{zx_{I-1,j}} - C^k_{zx_{I-2,j}}}{2h\,(k+1)} \quad j = 0, \cdots, J \tag{19}$$

$$\mu C^{k+1}_{zy_{i,0}} = \frac{-3C^k_{zy_{i,0}} + 4C^k_{zy_{i,1}} - C^k_{zy_{i,2}}}{2h\,(k+1)} \quad i = 0, \cdots, I \tag{20}$$

$$\mu C^{k+1}_{zy_{i,J}} = \frac{-3C^k_{zy_{i,J}} + 4C^k_{zy_{i,J-1}} - C^k_{zy_{i,J-2}}}{2h\,(k+1)} \quad i = 0, \cdots, I \tag{21}$$

where two-order difference schemes are used for one-order Mur's ABC.

3. Numerical Results

To show the good performance of the PML-ABC with implementation of the ATS-FDTD, three examples are given in this section. The conductivity σ in PML is defined as [1]

$$\sigma = \sigma_{max} \left(\frac{\rho}{d}\right)^m \tag{22}$$

where $\rho(\leq d)$ is the distance of PML layer from the inside PML interface. The reflection error at observation point in the time domain is defined as

$$\mathscr{E}|^n = 20 \log \left| \frac{\left|H_z^{PML} - H_z^{Ref.}\right|}{\max\left|H_z^{Ref.}\right|} \right|^n \tag{23}$$

where H_z^{PML} denotes the numerical results and $H_z^{Ref.}$ denotes the reference results, free of reflection errors and computed with a large enough domain. K and size of grid are calculated by (10).

Example I. In the first example, comparison between PML-ABC and the traditional PML, PML-PEC, is presented. The vacuum domain contains 101 × 101 cells and the time-harmonic source is located at the center of the vacuum. Observation point is located one cell diagonally away from a corner of the PML interface.

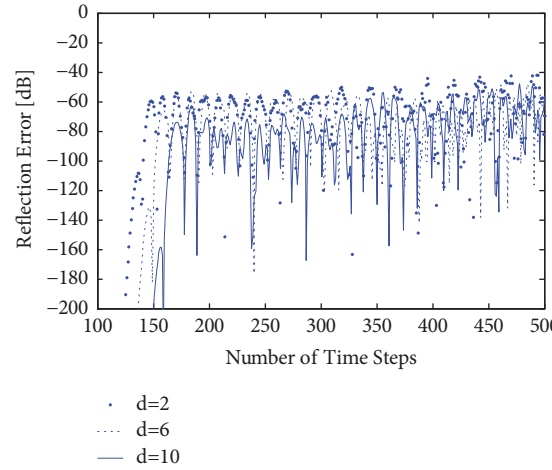

Figure 1: Reflection error of results of PML-ABC as a function of time step with m=2, σ_{max}=2.6e-8, f= 18.83(Hz), h=2000(m), Δt=3.35e-6(s), K=5, and varying d.

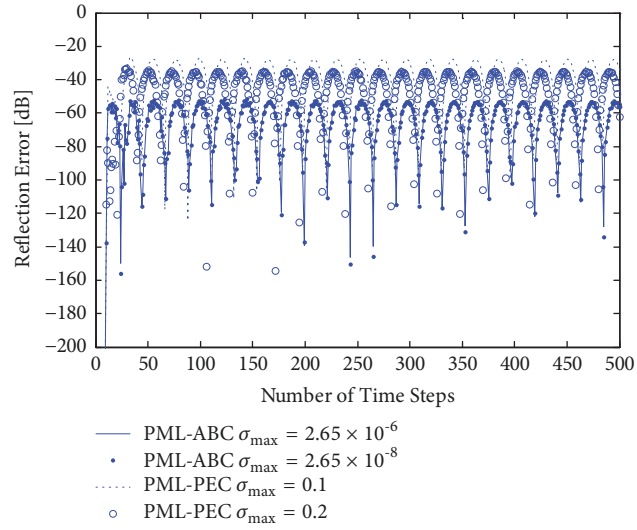

Figure 2: Reflection error of results of PML-ABC and PML-PEC as a function of time step with d=2, m=2, f=1.88e+11(Hz), h=0.01(m), Δt=2.37e-10(s), K=94, and varying σ_{max}.

Figures 1–3 show the reflection errors with varying variables where $H_z^{P.A.}$ denotes the numerical results computed with the PML-ABC boundary and $H_z^{P.P.}$ denotes the numerical results computed with the PML-PEC boundary. Figure 1 illustrates the reflection error of PML-ABC with different thick d. From Figure 1 we can find that the reflection error decline along with increasing d. Figure 2 shows comparison between PML-ABC and PML-PEC with different σ_{max}, where d=12 for PML-PEC. From Figure 2 we can find that the reflection errors of PML-ABC are less than that of PML-PEC. The performance of PML-ABC is slightly affected by σ_{max},

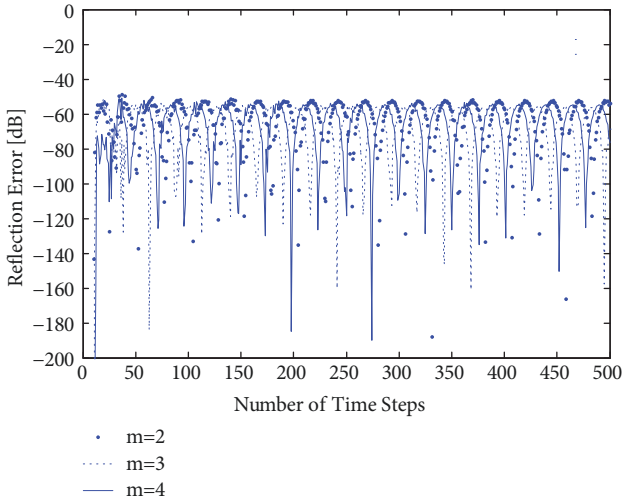

Figure 3: Reflection error of results of PML-ABC as a function of time step with d=2, σ_{max}=2.6e-7, f = 1.88e+17(Hz), h=2.0e-5(m), Δt= 4.34e-13(s), K=84, and varying m.

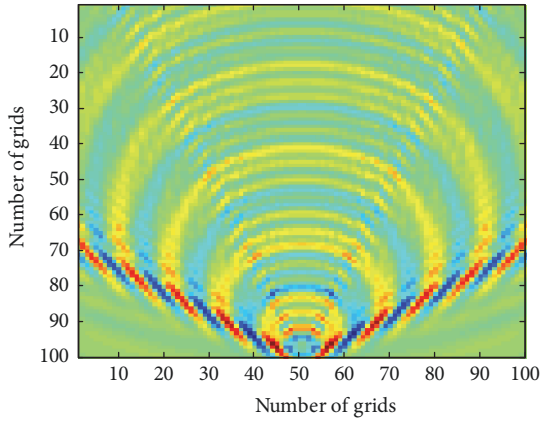

Figure 4: $\sqrt{\mu}H^n_{z_{i,j}}$ at time step n=32 for Example II.

while the performance of PML-PEC is distinctly affected by σ_{max}. Figure 3 shows the reflection errors of PML-ABC are slightly affected by power m.

Figures 1–3 illustrate the good performance of PML-ABC, reflection error around -60[dB], with only two PML layers.

Figures 4–7 show that the ATS-FDTD method works well with the PML-ABC.

Example II. The second example shows the good performance with a complex wave where time-harmonic source with frequency f= 1.43e+11(Hz) moves along x_{51} with speed $3m/ns$. And the vacuum domain contains 101×101 cells with d = 2, σ_{max}=0.083, h=1.0e-2(m), dt= 1.04e-10(s), K=86, and m = 3.

Figure 4 shows the numerical magnetic-field component at time steps n=32 where the outgoing wave does not cause an obvious echo from the PML-ABC. Figure 5 presents the error reflection around -60[dB] at point $A1(x_2, y_2)$ and $A2(x_{15}, y_{15})$.

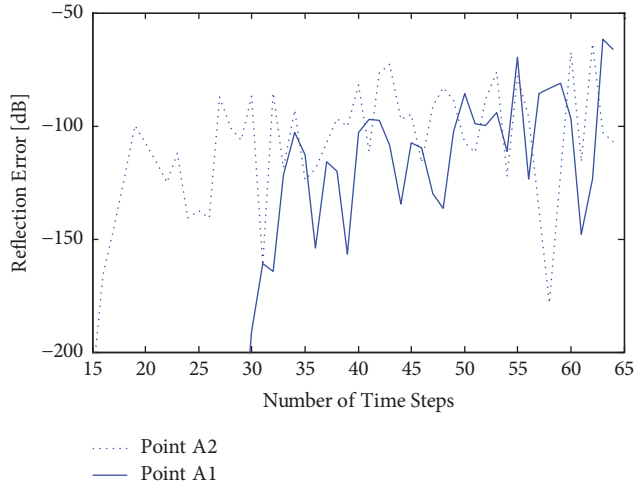

Figure 5: Reflection error as a function of time step for Example II.

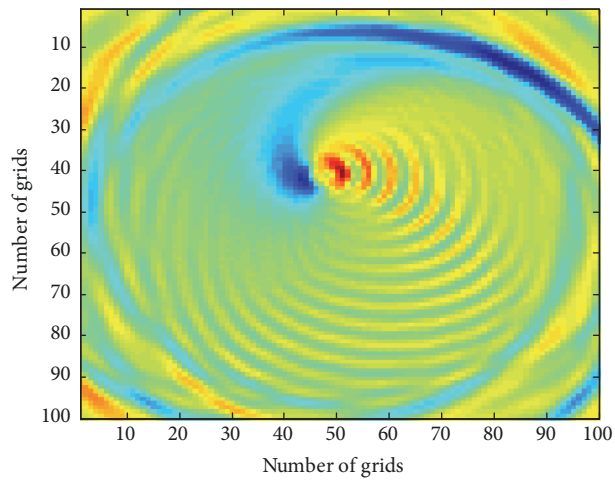

Figure 6: $\sqrt{\mu}H^n_{z_{i,j}}$ at time step n=20 for Example III.

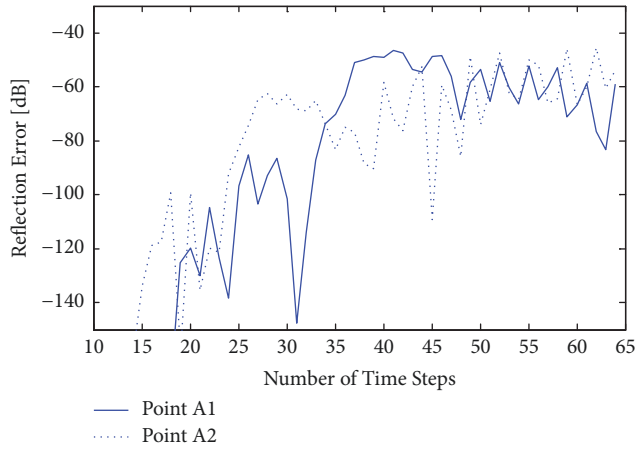

Figure 7: Reflection error as a function of time step for Example III.

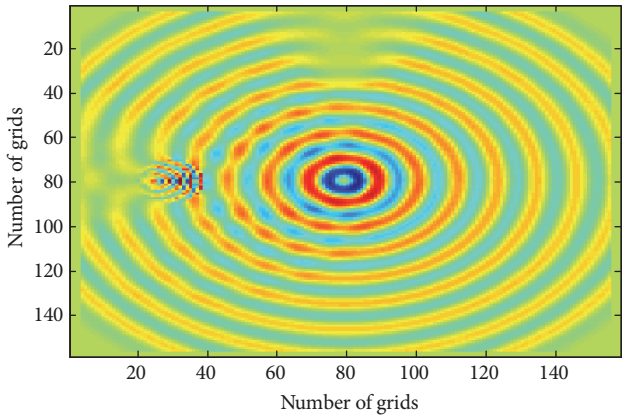

FIGURE 8: $\sqrt{\mu}H^n_{z_{i,j}}$ at time step n=100 for Example IV.

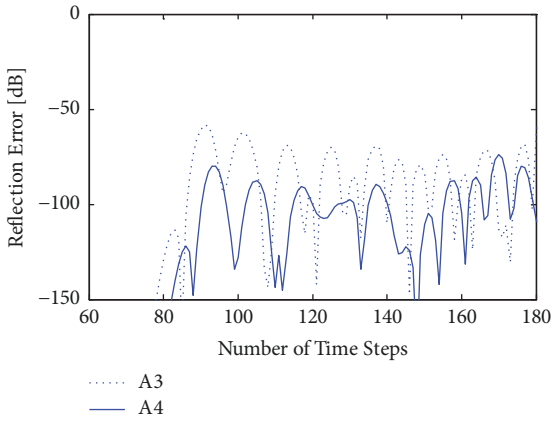

FIGURE 9: Reflection error as a function of time step for Example IV.

Example III. In the third example, variables and coefficients are the same as those in Example II. Here, three time-harmonic sources are placed around (x_{51}, y_{51}) with isogonal location and 10 cells away from center. With initial phases $0, 2\pi/3, 4\pi/3$, these three sources circle around (x_{51}, y_{51}) with angular speed of $(\pi/18)rad/ns$. Figure 6 presents the numerical magnetic-field component at time steps $n = 20$, where the complex outgoing wave goes through the PML-ABC and does not cause an obvious echo. Figure 7 shows reflection errors around -60[dB] at points A1 and A2.

Example IV. In the fourth example, variables and coefficients are the same as those in Example II while the vacuum domain contains 150×150 cell. Here, time-harmonic source is placed in the center. A circle with conductivity $\sigma = 10\pi\sqrt{\mu/\varepsilon}$ and 40 cells away from center is placed at (x_{75}, y_{35}). And a circle with electric permittivity 10.25ε and 40 cells away from center is placed at (x_{35}, y_{75}). Figure 8 presents the numerical magnetic-field component at time steps $n = 100$, where the complex outgoing wave goes through the PML-ABC and does not cause an obvious echo. Figure 9 shows reflection errors around -60[dB] at points A3 (x_2, y_{75}) and A4 (x_{75}, y_2).

4. Conclusions

This paper presents a well-designed termination wall for PML on staggered grid where all electromagnetic field components are placed on the boundary of each cell. Numerical experimentations show that the PML-ABC works well with ATS-FDTD method to solve Maxwell equation in free-domain. The PML-ABC can be decreased to two layers with reflection error -60[dB] when simulate complex waveguide.

Data Availability

No data were used to support this study.

Ethical Approval

This article does not contain any studies with human participants or animals performed by any of the authors.

Conflicts of Interest

All authors declare that they have no conflicts of interest.

Acknowledgments

The work was supported by the National Natural Science Foundation of China (11571367), Shandong Provincial Natural Sciences Foundation (ZR2014AM029, ZR2015AL006), and China Scholarship Council Foundation (Grant no. 201806455012).

References

[1] J. Berenger, "A perfectly matched layer for the absorption of electromagnetic waves," *Journal of Computational Physics*, vol. 114, no. 2, pp. 185–200, 1994.

[2] W. C. Chew and W. H. Weedon, "A 3-D perfectly matched medium for the modified Maxwell equations with stretched coordinates," *Microwave & Optical Technology Letters*, vol. 7, no. 13, pp. 257–260, 1994.

[3] Q.-H. Liu and J. Tao, "The perfectly matched layer for acoustic waves in absorptive media," *The Journal of the Acoustical Society of America*, vol. 102, no. 4, pp. 2072–2082, 1997.

[4] A. Fathi, B. Poursartip, and L. F. Kallivokas, "Time-domain hybrid formulations for wave simulations in three-dimensional PML-truncated heterogeneous media," *International Journal for Numerical Methods in Engineering*, vol. 101, no. 3, pp. 165–198, 2015.

[5] B. Chen, D. G. Fang, and B. H. Zhou, "Modified Berenger PML absorbing boundary condition for FD-TD meshes," *IEEE Microwave and Guided Wave Letters*, vol. 5, no. 11, pp. 399–401, 1995.

[6] J. Berenger, "Improved PML for the FDTD solution of wave-structure interaction problems," *IEEE Transactions on Antennas and Propagation*, vol. 45, no. 3, pp. 466–473.

[7] E. Margengo, C. Rappaport, and E. Miller, "Optimum PML ABC conductivity profile in FDFD," *IEEE Transactions on Magnetics*, vol. 35, no. 3, pp. 1506–1509.

[8] C. M. Rappaport, "Interpreting and improving the PML absorbing boundary condition using anisotropie lossy mapping of

space," *IEEE Transactions on Magnetics*, vol. 32, no. 3, pp. 968–974, 1996.

[9] Y. S. Rickard, N. K. Georgieva, and W. P. Huang, "Application and optimization of PML ABC for the 3-D wave equation in the time domain," *IEEE Transactions on Antennas & Propagation*, vol. 51, no. 2, pp. 286–295, 2003.

[10] Y. S. Rickard and N. K. Georgieva, "Problem-Independent Enhancement of PML ABC for the FDTD Method," *IEEE Transactions on Antennas and Propagation*, vol. 51, no. 10, pp. 3002–3006, 2003.

[11] Y. S. Rickard and N. K. Nikolova, "Enhancing the PML absorbing boundary conditions for the wave equation," *IEEE Transactions on Antennas and Propagation*, vol. 53, no. 3, pp. 1242–1246, 2005.

[12] R. Shi, H. Yang, and L. Gao, "An adaptive time step FDTD method for Maxwells equations," *IEEE Antennas & Wireless Propagation Letters*, vol. 14, pp. 1706–1709, 2015.

[13] K. S. Yee, "Numerical solution of initial boundary value problems involving Maxwells equations in isotropic media," *IEEE Transactions on Antennas & Propagation*, vol. 14, no. 3, pp. 302–307, 1966.